UNCLASSIFIED

AD NUMBER

AD859279

NEW LIMITATION CHANGE

TO

Approved for public release, distribution unlimited

FROM

Distribution authorized to U.S. Gov't. agencies only; Administrative/Operational Use; JUL 1969. Other requests shall be referred to Naval Civil Engineering Lab., Port Hueneme, CA 93041.

AUTHORITY

Naval Civil Engineering Lab. ltr dtd 27 Apr 1970

THIS PAGE IS UNCLASSIFIED

AD 859279

Technical Note N-1042

CORROSION OF IRON IN 0.5M NaCl - A ROTATING DISK ELECTRODE STUDY

By

Howard A. Porte

July 1969

DDC
SEP 25 1969

Each transmittal of this document outside the agencies of the U. S. Government must have prior approval of the Naval Civil Engineering Laboratory.

NAVAL CIVIL ENGINEERING LABORATORY
Port Hueneme, California 93041

36

CORROSION OF IRON IN 0.5M NaCl - A ROTATING DISK ELECTRODE STUDY

Technical Note N-1042

Z-R011-01-01-035

by

Howard A. Porte

ABSTRACT

The corrosion of iron was studied in 0.5 Molar sodium chloride solution by the rotating disk technique. Limiting diffusion currents were measured in nitrogen-saturated, air-saturated, and oxygen-saturated solutions at rotational speeds of 0, 100, 400, 900, 1600 and 2500 rpm. Corrosion potentials and corrosion rates at the corrosion potential were also determined. The observed limiting diffusion currents showed good agreement with limiting diffusion currents calculated from the Levich theory for the rotating disk electrode. Measured corrosion rates (currents) were found to be lower than the limiting diffusion current, which is explained on the basis of a corrosion product film on the surface of the electrode.

ACCESSION for
CFSTI WHITE SECTION
DDC BUFF SECTION
UNANNOUNCED
JUSTIFICATION
BY
DISTRIBUTION/AVAILABILITY CODES
DIST. AVAIL. and/or SPECIAL
3

Each transmittal of this document outside the agencies of the U. S. Government must have prior approval of the Naval Civil Engineering Laboratory

INTRODUCTION

The corrosion of iron and steel in aqueous environments, especially seawater, still remains a problem, the importance and complexity of which is attested to by the vast literature in the field. And, although many corrosion rate studies have been conducted in seawater, few have been concerned with correlating the effects of environmental variables, whether singly or synergistically, with observed corrosion rates. The most important environmental variables, from the corrosion standpoint, are dissolved oxygen concentration, flow velocity and temperature. Other factors which exert varying influence on the corrosion rate are pH, salinity, biological species, duration of exposure, and the presence of suspended matter.

The corrosion of iron in aqueous solution is electrochemical in nature consisting of an anodic reaction, equation (1), and a cathodic reaction. In the absence of oxygen the cathodic reaction is represented by equation (2a) or (2b):

$$Fe = Fe^{++} + 2e \qquad (1)$$

$$2H^{+} + 2e = H_2, \text{ in acid media or} \qquad (2a)$$

$$2H_2O + 2e = H_2 + 2OH^{-} \text{ in alkaline media} \qquad (2b)$$

In the presence of oxygen the principle cathodic reaction is represented by equation (3a) or (3b):

$$\tfrac{1}{2}O_2 + H_2O + 2e = 2OH^{-} \text{ in alkaline media} \qquad (3a)$$

$$2H^{+} + \tfrac{1}{2}O_2 + 2e = H_2O \text{ in acid media} \qquad (3b)$$

The overall reactions in an oxygen-free neutral solution can be formed by combining equations (1) and (2b):

$$Fe + 2H_2O = Fe(OH)_2 + H2 \qquad (4)$$

At ordinary temperatures the reaction shown in equation (4) takes place at very slow rates in an oxygen-free neutral solution and hence a negligible amount of corrosion occurs.

The overall reaction taking place in a neutral solution containing oxygen is formed by combining equations (1) and (3a):

$$Fe + \frac{1}{2}O_2 + H_2O = Fe(OH)_2 \quad (5)$$

The reduction of oxygen at cathodic sites takes place rapidly so that oxygen concentration on the iron surface approaches zero; thus, the rate limiting step for the corrosion process is seen to be the diffusion of oxygen from the bulk solution to the metal surface. The limiting diffusion current for oxygen then seems to correspond to the maximum corrosion rate. If the corrosion film acts as a barrier to diffusion, the corrosion rate would be lower than this limiting value and would vary with the thickness of the corrosion film. The changes often observed in corrosion rate over a period of time are usually primarily due to changes in the porosity and thickness of the corrosion film. These electrochemical principles of corrosion can be readily visualized by reference to the schematic polarization diagram for iron in aqueous solution shown in Figure 1. Point F represents the reversible potential of the iron electrode. At this reversible potential the rate of oxidation of metal, $Fe = Fe^{++} + 2e$, equals the rate of reduction of metal ions, $Fe^{++} + 2e = Fe$, and the current corresponding to this rate is called the exchange current for the iron electrode. Points H and O represent the reversible potentials for the hydrogen and oxygen electrodes, respectively. When corrosion occurs in the absence of oxygen, iron is oxidized and hydrogen ions are reduced until a steady-state is reached at Point C; the potential at C is called the corrosion potential, $E_{corr(1)}$, and the current is called the corrosion current, $I_{corr(1)}$. In the presence of oxygen an additional reduction reaction, such as equation (3b), takes place. However, at high currents diffusion limits the rate at which oxygen can arrive at the electrode and the electrode potential changes sharply until a potential is reached where a new reaction proceeds. For the corroding iron system, the intersection of the anodic iron polarization curve with the oxygen reduction curve gives a new corrosion potential, $E_{corr(2)}$, and a new corrosion current, $I_{corr(2)}$.

Applying a cathodic current to the corroding system where oxygen is present would give the cathodic polarization curve marked P_2; for the system where oxygen is absent the cathodic polarization curve P_1 is obtained. The portions of curve P_2 where the potential changes sharply is known as the limiting diffusion current and corresponds to the maximum rate at which oxygen can diffuse to the electrode surface which is proportional to the maximum corrosion rate. From the corrosion scientist's standpoint it is important to know what the limiting diffusion is for a system and how changes in the environment will affect the limiting diffusion current. In this study the rotating disk technique was used to measure the limiting diffusion currents for oxygen diffusion in air-saturated, oxygen-saturated, and nitrogen-saturated 0.5 molar aqueous sodium chloride solution (0.5M NaCl). Also, a rotating Armco iron disk was employed to measure the corrosion rate by the "polarization resistance" method. The effects of velocity and dissolved oxygen concentration on the anodic and cathodic polarization curves and the corrosion potential were also determined.

EXPERIMENTAL APPARATUS

The cell was a 1 liter beaker with a lucite top containing 5 holes which allowed insertion of the working electrode, saturated calomel reference electrode, platinum counter electrode, thermometer, and fitted glass bubbling tube. The working electrode was fabricated from a ½-inch diameter Armco iron rod cut into cylindrical electrodes approximately ½ inch in length. All but the lower face of the electrode was covered by a teflon sleeve. The lower face exposed to the solution, approximately 1¼ square centimeters in area, was wet-polished (demineralized water as lubricant) with succeeding finer grades of silicon-carbide paper through No. 600, degreased with acetone and finally rinsed with demineralized water prior to insertion in the cell. The analysis of the Armco iron used for the electrodes is:

C - 0.020%
Mn - 0.044%
P - 0.003%
S - 0.018%
Si - 0.004%
Cu - 0.92%
Fe - Balance

These data were obtained by Fagersta Steels Pacific, Incorporated, Los Angeles, California and supplied by the manufacturer.

The rotating shaft was a 7/16-inch diameter steel rod, 15 inches long. Eccentric motion was held to a minimum by two precision ball bearings placed in the holder by which the assembly was clamped. The cylindrical electrode was screwed into the bottom of the shaft. Electrical contact was made by means of a spring-tensioned carbon brush. The rotating shaft was coupled to the stirring motor by means of a polyethylene insulator at the upper end of the shaft. The power for rotation was supplied by a Bodine Model NSH-34 DC motor and a Minarik Model SH speed control. Rotational speeds were measured with an electronic stroboscope. The electrochemical polarization was performed with an electronic potentiostat, Wenking Model 61-TR; potential sweep rates of 4 volts/hr were generated by feeding the output from an Erwin Halstrup Model MP-64 motor potentiometer into the potentiostat. Potentials were measured with a Keithley Model 610B electrometer with an input impedence of 10^{14} ohms. Current was determined by measuring the voltage drop across a precision 1 ohm resistor; for recording purposes the voltage drop was then amplified with a Dana Model 3850 DC amplifier. Current and potential were recorded simultaneously on (1) a Leeds and Northrup Speedomax G 2-pen recorder, and (2) an Ampex Series 800B tape recorder. The polarization curves were obtained by converting the data on magnetic tape to punched cards via an analog-to-digital converter and an IBM 1620 II computer; a special FORTRAN II program and an IBM 1627 plotter then produced the curves.

The 0.5M NaCl solution was made from Baker "Analyzed Reagent" grade sodium chloride and deionized water.

In order to insure saturation of the solution (nitrogen, air, or oxygen) gas flow was started 16 hours before inserting the electrode assembly and continued throughout the experiment. The polarization cell was immersed in a constant temperature bath so that all experiments were performed at 25 ± 1°C. The electrode was allowed to come to a steady-state corrosion potential before cathodic polarization was started. The cathodic polarization curves were obtained over the range from the corrosion potential to -1400 mv vs. S.C.E. Current values are obtained continuously on both tape and the strip chart recorder as a function of a changing applied potential.

RESULTS AND DISCUSSION

Corrosion is a heterogeneous reaction involving five principal steps:

(1) Transport of reactant molecules or ions to the electrode surface.

(2) Adsorption at the surface.

(3) An electron transfer reaction at the surface,

(4) Desorption from the surface.

(5) Transport of reaction products away from the surface.

For the corrosion of iron in aqueous solution, step (1) is the slowest, and thus the rate-controlling step, in the overall corrosion reaction. The transport of oxygen to the electrode surface is controlled primarily by the velocity of the solution (or electrode) and the concentration of dissolved oxygen. These effects are shown qualitatively in Figure 2. Curve (1) represents the situation for some initial conditions of concentration and velocity. Curve (2) shows the effect of increasing the concentration but keeping the velocity constant. Curve (3) shows the change in limiting current density when the velocity is increased but the concentration remains constant. It is of course desirable to have an analytical relationship between limiting diffusion current, velocity, and concentration so that the limiting diffusion current resulting from changes in velocity or concentration can be calculated. An early attempt to explain the effects of velocity and concentration in the diffusion current density was given by Nernst as expressed in equation (6), below:

$$i_d = nDF \frac{C_b - C_s}{\delta} \qquad (6)$$

where

i_d is the diffusion current density, n is the number of electrons in the electron-transfer reaction

D is the diffusion coefficient of oxygen

F is the Faraday

C_∞ is the concentration of dissolved oxygen in the bulk of the solution

C_o is the concentration of dissolved oxygen at the interface

δ is the thickness of the diffusion layer

For the situation where the concentration of dissolved oxygen at the interface becomes zero, then i_d becomes the limiting diffusion current. It is apparent that the limiting diffusion current will increase as δ becomes thinner. However, a major shortcoming of Nernst's treatment is that there is no way of predicting how δ will be affected by the changes in velocity. The problem of mass transfer to a rotating disk was solved by Levich. The treatment yields the following solution for the limiting current density:

$$i_{lim\,d} = 0.620\ nFDC_\infty \left(\frac{\nu}{D}\right)^{1/3} \left(\frac{\omega}{\nu}\right)^{1/2} \qquad (7)$$

where ω is the angular velocity of the disk and ν is the kinematic viscosity of the solution. The expression is seen to relate the six quantities $i_{lim\,d}$, n, D, C_∞, ν and ω, any one of which may be determined if the other five are known. In practice ν and ω are best determined directly. The thickness of the Nernst diffusion layer may be determined from the Levich equation since it is, in this case

$$\delta = 1.62 \left(\frac{D}{\nu}\right)^{1/3} \left(\frac{\nu}{\omega}\right)^{1/2} \qquad (8)$$

Thus δ may be calculated for any rotational speed. The Levich treatment is of course only applicable where the flow is laminar. This is one of the advantages of the rotating disk system since turbulence does not set in until the Reynolds number is about 10^5. For non-streamlined electrodes, such as cylinders, the flow becomes turbulent at Reynolds' numbers of only 200. Another advantage of the rotating disk system is that δ, the diffusion layer thickness, is constant over the entire surface of the disk.

This study was concerned with the determination of (1) limiting diffusion currents of oxygen, (2) corrosion rates of iron, and (3) corrosion potential of iron, each as a function of velocity and dissolved oxygen concentration in 0.5M NaCl solution.

Limiting Diffusion Currents of Oxygen

The limiting diffusion current of oxygen to an iron electrode is of importance because it is proportional to the maximum rate at which the iron can corrode. Experimentally, the limiting diffusion current may be obtained from the cathodic polarization curve. Comparison of the experimentally determined limiting diffusion currents with those calculated from the Levich theory for a rotating disk then allows interpretation of the corrosion mechanism. As a basis of comparison, cathodic polarization curves were made for Armco iron in nitrogen-saturated 0.5M NaCl at 25°C. These curves at rotational speeds of 0, 100, 400, 900, 1600 and 2500 are shown in Figures 3 to 8. Since oxygen is not present, the cathodic reaction occuring on the electrode is the reduction of hydrogen ions, $2H^+ + 2e > H_2$. As expected, no region of limiting current is observed and the curves are nearly identical at all rotational speeds since the rate of the reaction is controlled by the electron-transfer step rather than mass transport of reactant to the interface. The linear portion of the curves occuring at potentials more negative than ca. - 900 mv are referred to as the Tafel regions since the overvoltage curve corresponds to the Tafel equation

$$\epsilon = -\beta_c \log \frac{i}{i_{corr}}$$

where ϵ is the overvoltage, β_c is the cathodic Tafel slope, i is the applied current, and i_{corr} is the corrosion current.

Cathodic polarization curves for Armco iron in air-saturated 0.5M NaCl are shown in Figures 9 through 14. It will be observed that the polarization curve at 0 rpm (stationary) is quite erratic in the limiting diffusion region, which is probably caused by a non-uniform flow of oxygen to the electrode since transport is primarily by natural convection and because the diffusion layer is not of uniform thickness under these conditions. At the higher rotational speeds, where transport is due to forced convection, smooth polarization curves are obtained. The portion of the curves where the current remains nearly constant represents the limiting diffusion region. As predicted by the Levich theory, the limiting diffusion currents increase with increasing rotational speeds. At the speed of zero (stationary), mass transport to the interface is controlled by natural convection. In the limiting diffusion region, the principal reduction reaction occuring on the surface is the reduction of oxygen by $4H^+ + O_2 + 4e\ 2H_2O$. At highly negative potentials, i.e., more negative than ca. - 1200, the hydrogen reduction reaction becomes predominant and the curve follows the hydrogen Tafel slope.

The current goes through the smallest change in the region -800 to -1000 mv and for comparison purposes the limiting diffusion currents were read at -900 mv. These currents are listed in the column headed $i_{lim\ d}$ (Table 1).

Cathodic polarization curves for Armco iron in oxygen-saturated 0.5M NaCl at rotational speeds of 0 to 2500 rpm are shown in Figures 15 through 20. Similar to the curves for air-saturated solution, a relatively flat portion is seen in the limiting diffusion region. The hydrogen evaluation region begins at ca. -1100 mv at 0 rpm and decreases to ca. -1200 at 2500 rpm. At a given rotational speed, limiting diffusion currents are larger in oxygen-saturated solution than in air-saturated solution, due to increased dissolved oxygen concentration.

Corrosion Potentials and Corrosion Currents at the Corrosion Potential

Prior to each cathodic polarization experiment the electrode was allowed to come to a steady-state corrosion potential; these potentials are listed (E_{corr}) in Table 1. Corrosion potentials in oxygen-saturated 0.5M NaCl ranged from -546 at 2500 rpm to -623 at 0 rpm. In air-saturated 0.5M NaCl the range was from -565 at 2500 rpm to -694 at 0 rpm. Data are given for six air-saturated experiments in addition to those corresponding to Figures 9 to 14; these illustrate the degree of reproducibility obtained. The range of corrosion potentials in nitrogen-saturated 0.5M NaCl was from -712 at 2000 rpm to -747 at 0 rpm. In general, corrosion potentials became less negative with increasing rotational speed and with increasing dissolved oxygen concentration, although in the nitrogen-saturated solutions the corrosion potentials were not as sensitive to changes in rotational speed. Corrosion currents were measured at the corrosion potential by the "polarization resistance" technique; the change in current was measured when the potential was polarized 10 mv from the corrosion potential and the corrosion current was measured from the relationship

$$\Delta E/\Delta I = \frac{B_a B_c}{2.3\ I_{corr}\ (B_a + B_c)}$$

where ΔE is the change in potential from the corrosion potential, ΔI is the corresponding change in current, B_a and B_c are the Tafel slopes and I_{corr} is the corrosion current. Corrosion currents calculated from this relationship are listed in Table 1. Corrosion currents are seen to increase with increasing rotational speed and with higher dissolved oxygen concentration. In the nitrogen saturated solution, corrosion currents were quite small, as would be expected, and not particularly sensitive to rotational speeds.

Comparison of Experimental Results with Levich Theory

On the basis of the Levich theory of the rotating disk electrode, equation (7), the limiting diffusion current should be proportional to the square root of the angular velocity. To test this theory the experimentally determined limiting diffusion currents (per unit area) in air-saturated 0.5M NaCl were plotted versus $(RPM)^{\frac{1}{2}}$ as shown in Figure 21. The dotted line in the figure represents the values calculated from the Levich equation,

$$i_{lim\ d} = 0.620\ nFDC_{\infty}\left(\frac{\nu}{D}\right)^{1/3}\left(\frac{\omega}{\nu}\right)^{\frac{1}{2}}$$

where

$$n = 4,\ F = 96,\ 500\ \frac{coul}{eq.},\ D = 2.0 \times 10^{-5}\ \frac{cm^2}{sec},$$

$$C_{\infty} = 2.0 \times 10^{-7}\ \frac{mole}{cm^3},\ \nu = 1.0 \times 10^{-2}\ \frac{cm^2}{sec}$$

The calculated limiting diffusion coefficients and the Nernst diffusion layer thicknesses calculated from the Levich equation for air-saturated 0.5M NaCl are listed in Table 2.

The observed limiting diffusion currents, shown in Figure 21 as circles, are seen to be in good agreement with calculated values between 100 and 1600 rpm. At 0 rpm the observed current is not zero as predicted by the Levich equation, but at a positive value due to mass transport by natural convection. At 2500 rpm, the observed current is also higher than calculated; in this region the deviation is probably due to some turbulence on the disk at the higher speed. The Reynolds number at 2500 rpm is 1.1×10^4 and since the surface is somewhat roughened due to a corrosion film, it is likely that the turbulent flow region is achieved.

The corrosion currents calculated by the polarization resistance" technique are shown in Figure 21 as triangles. The values show a dependence on $(RPM)^{\frac{1}{2}}$ but are all lower than the observed limiting diffusion currents. This is reasonable since the observed limiting diffusion currents represent the maximum rate at which the Armco iron could corrode and the "polarization resistance" currents represent actual corrosion rates with a corrosion product film on the surface. The corrosion product film on the surface represents an additional resistance to oxygen diffusion which slows down the corrosion rate from the limiting diffusion current. Thus, for iron with an oxide-free surface, the corrosion rate would be expected to approach the maximum value, i.e., the limiting diffusion current; however, as an intact corrosion product film builds up on the surface, the rate will decrease with time as the corrosion product film increases in thickness.

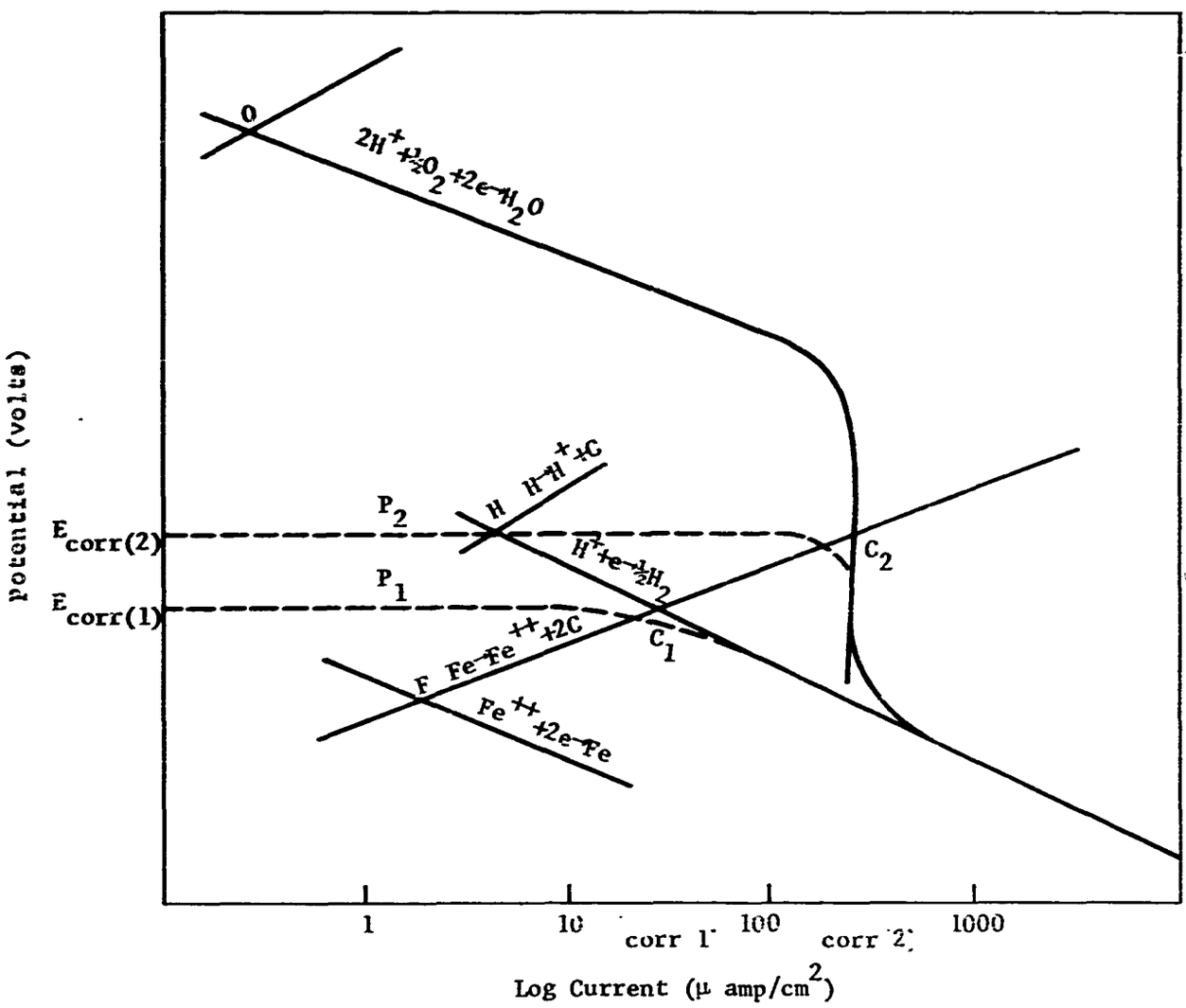

Figure 1. Schematic polarization diagram for iron corroding in aqueous solution.

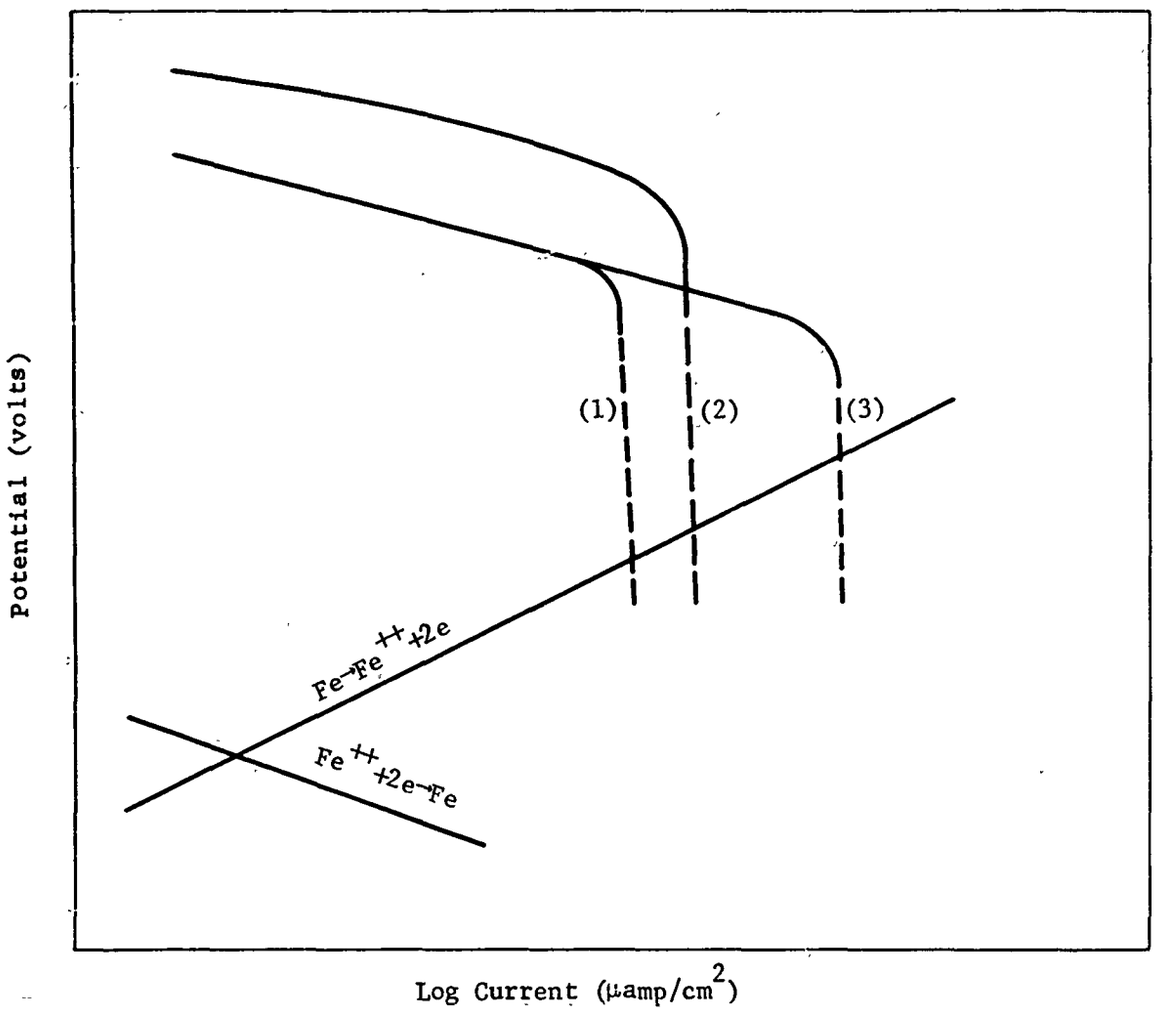

Figure 2. Schematic polarization diagram for iron in aqueous solution with transport of oxygen to electrode controlling the reaction.

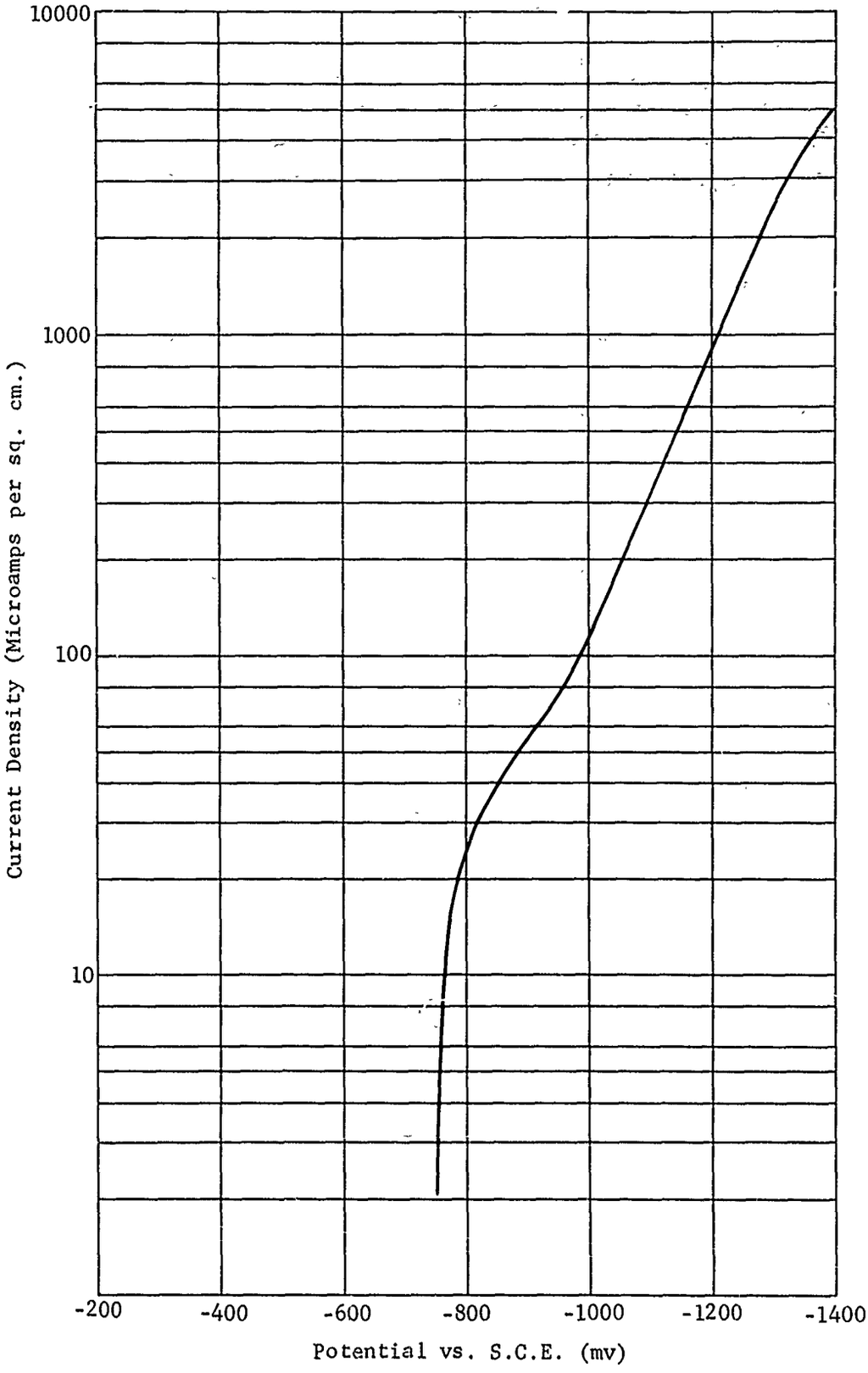

Figure 3. Cathodic polarization for armco iron in nitrogen-saturated aqueous 0.5M sodium chloride solution at 25°C; rotational speed of electrode = 0 rpm.

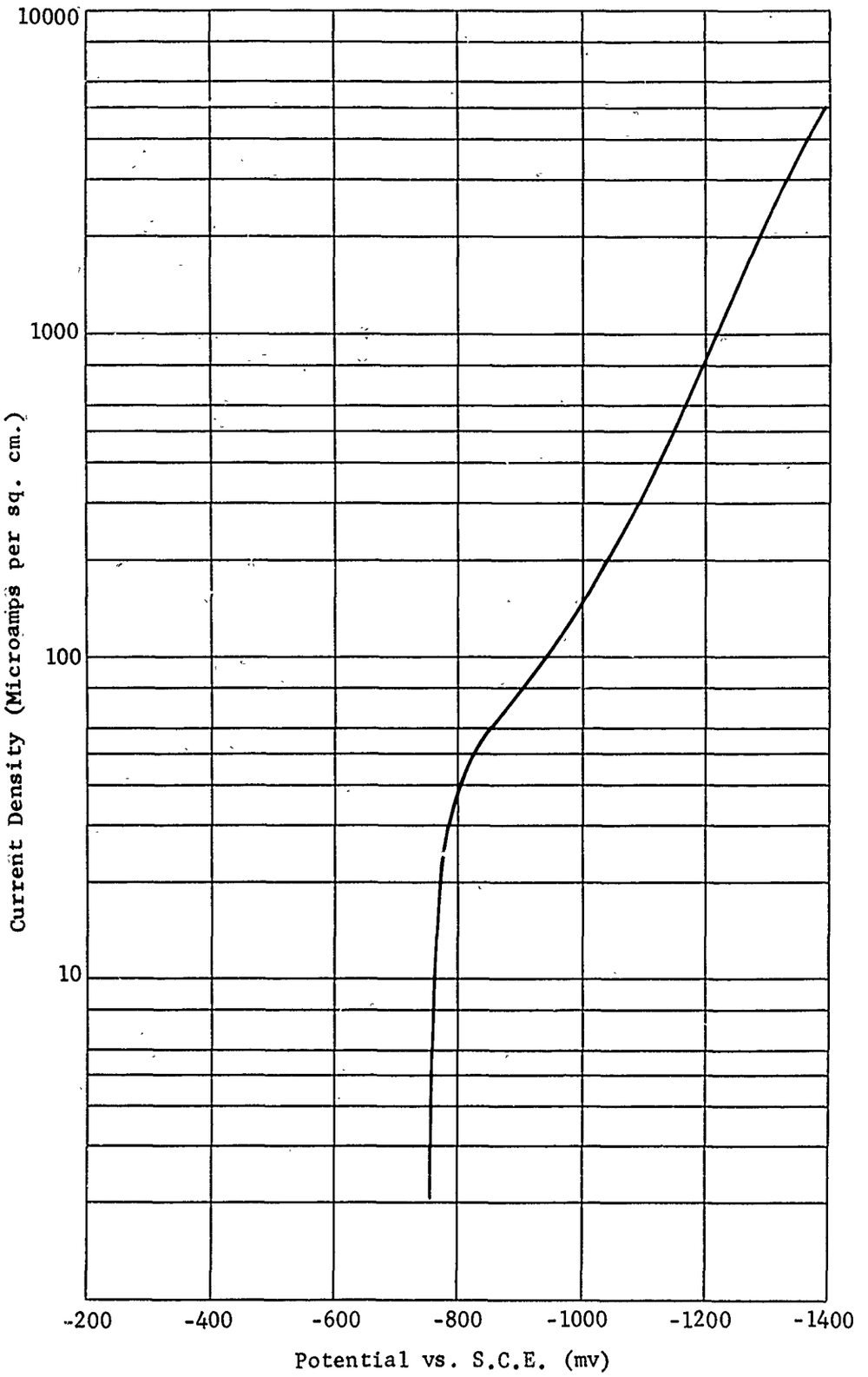

Figure 4. Cathodic polarization curve for armco iron in nitrogen-saturated aqueous 0.5M sodium chloride solution at 25°C; rotational speed of electrode = 100 rpm.

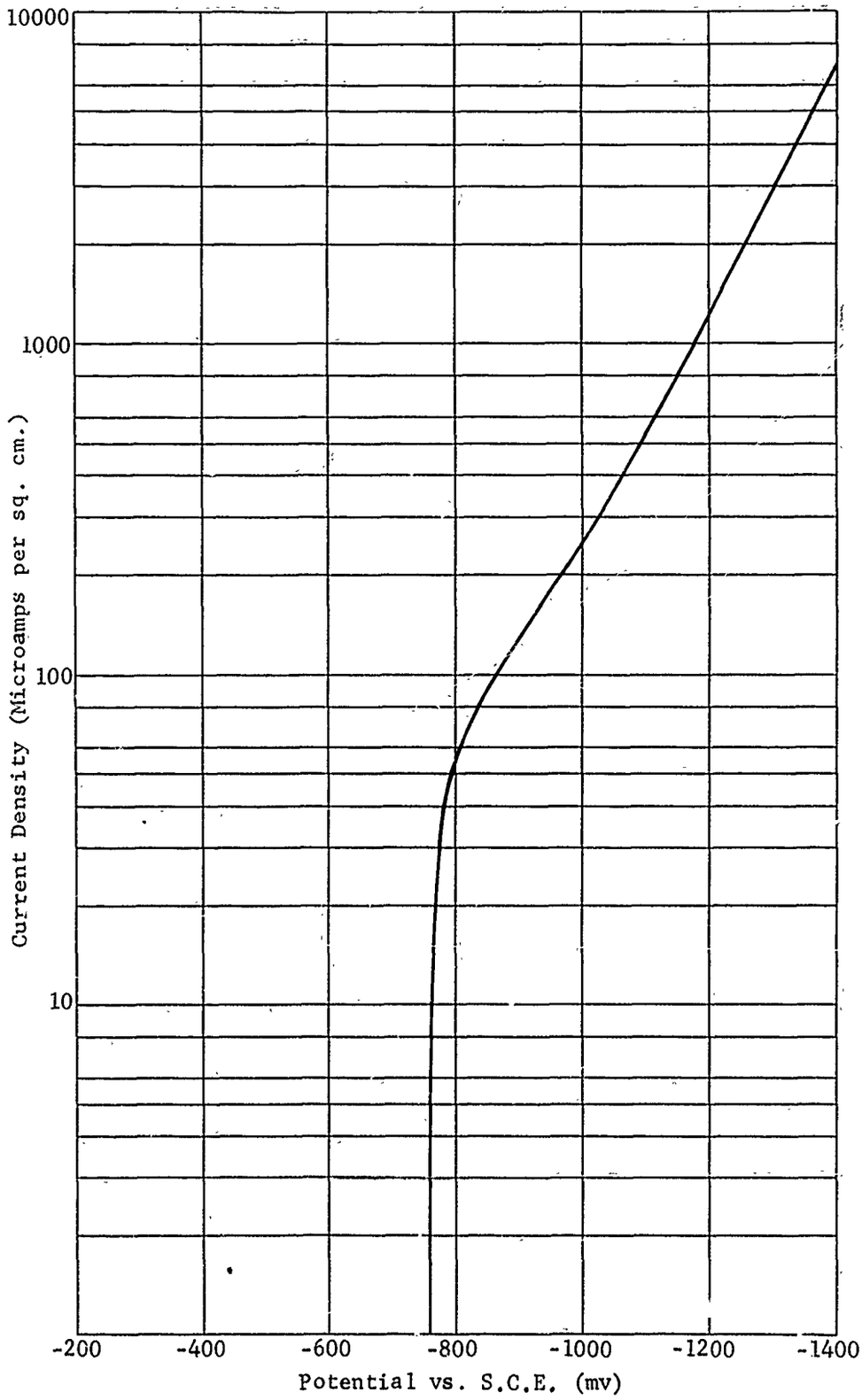

Figure 5. Cathodic polarization curve for armco iron in nitrogen-saturated aqueous 0.5M sodium chloride solution at 25°C; rotational speed of electrode = 400 rpm.

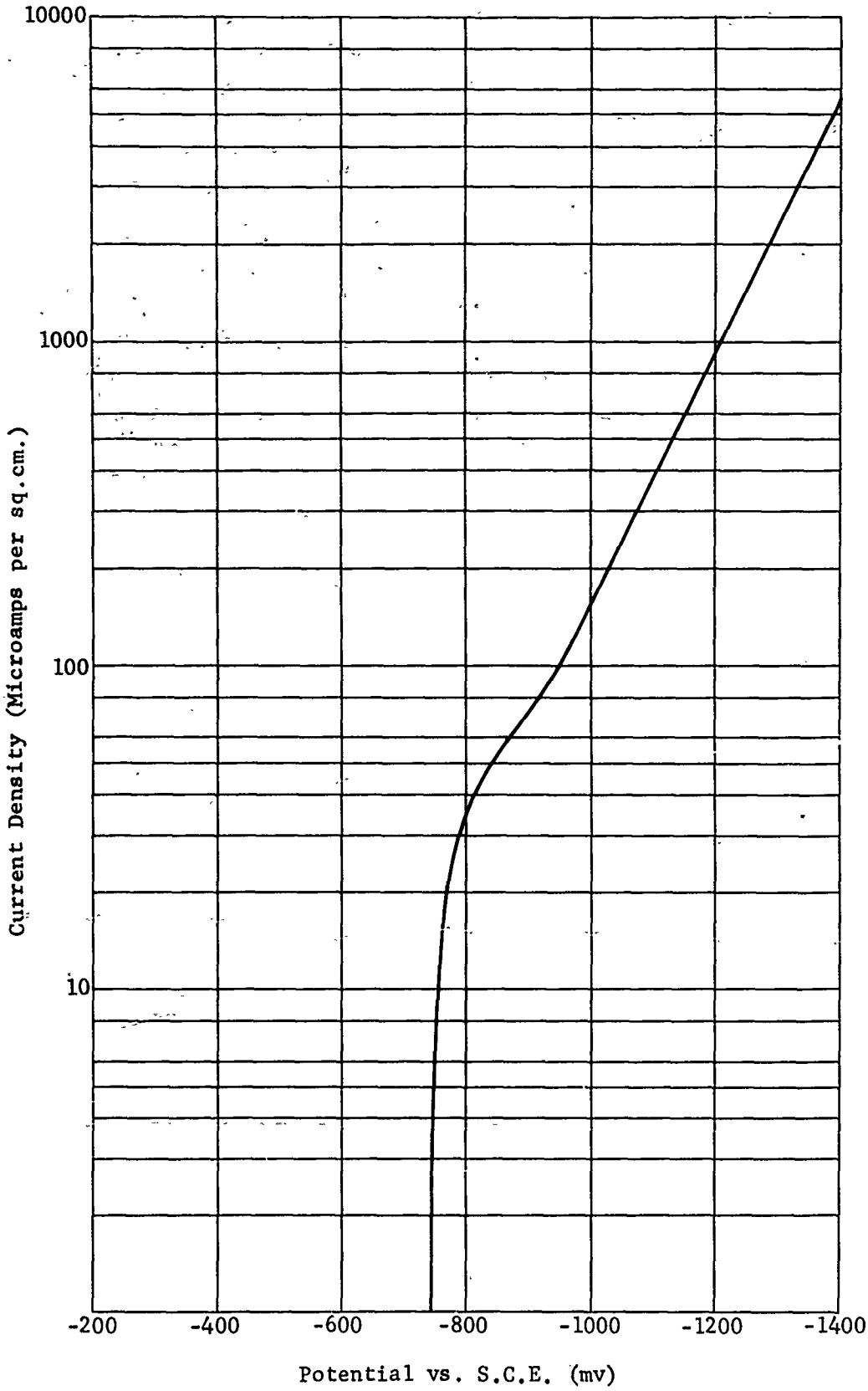

Figure 6. Cathodic polarization curve for armco iron in nitrogen-saturated aqueous 0.5M sodium chloride solution at 25°C; rotational speed of electrode = 900 rpm.

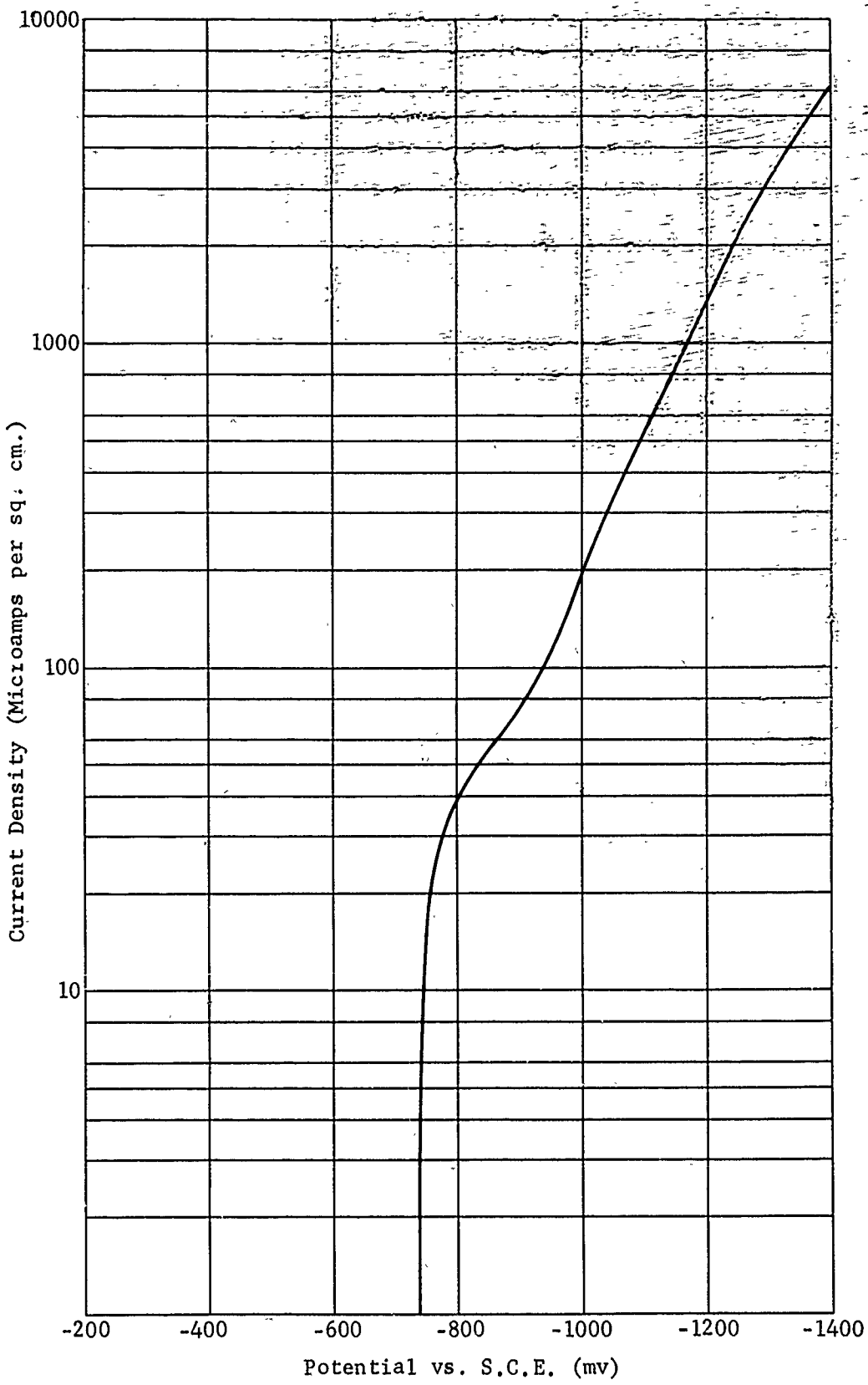

Figure 7. Cathodic polarization curve for armco iron in nitrogen-saturated aqueous 0.5M sodium chloride solution at 25°C; rotational speed of electrode = 1600 rpm.

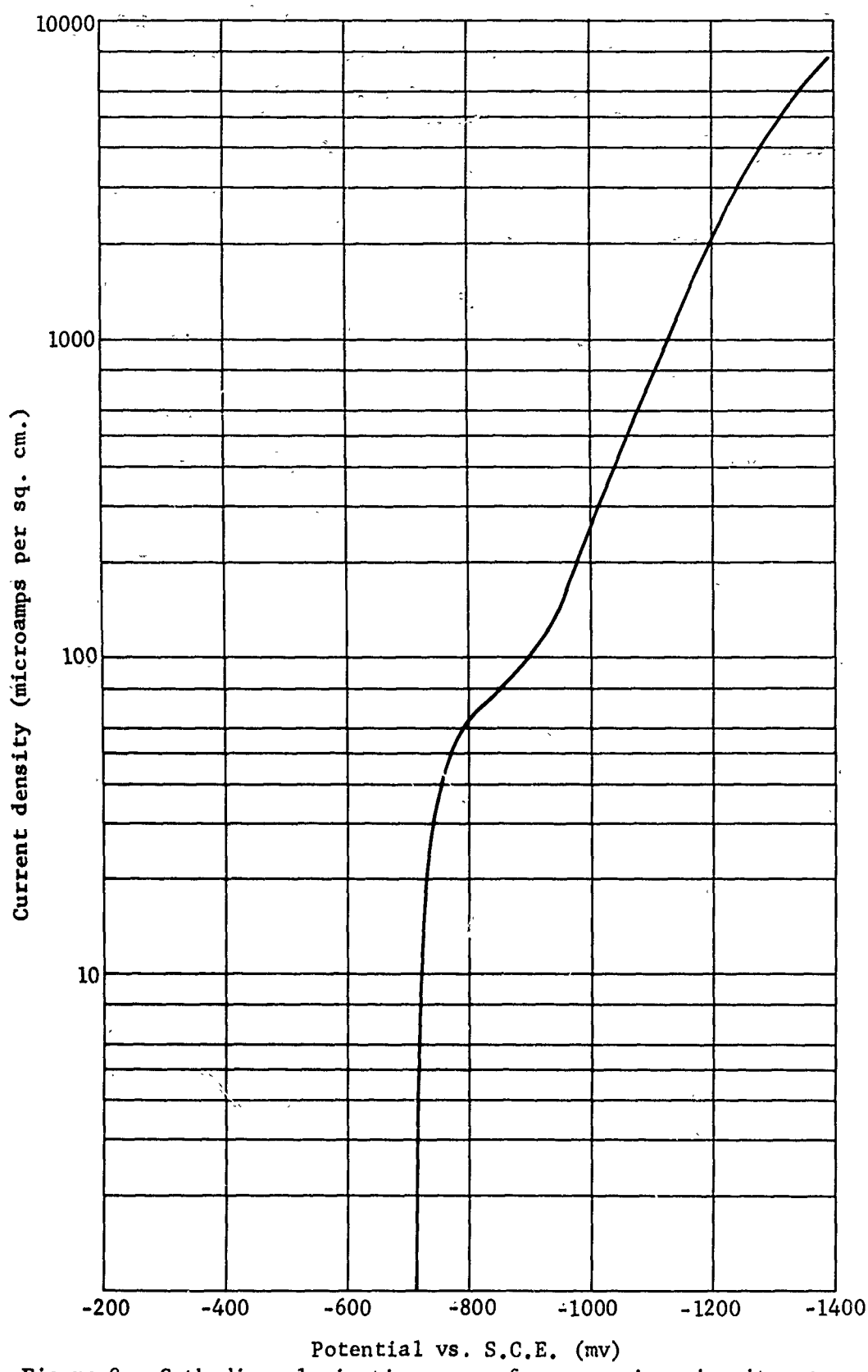

Figure 8. Cathodic polarization curve for armco iron in nitrogen-saturated aqueous 0.5M sodium chloride solution at 25°C; rotational speed of electrode = 2500 rpm.

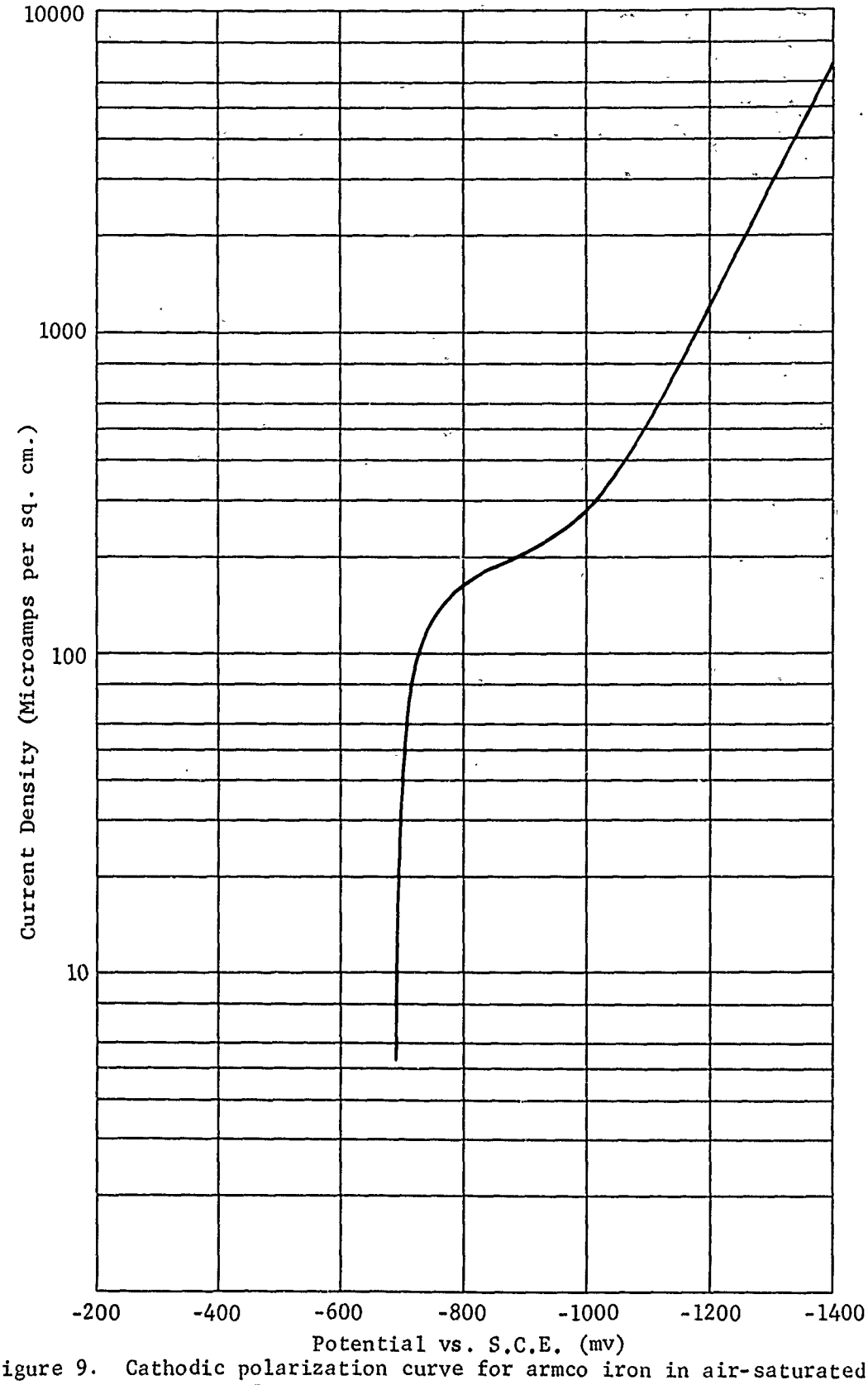

Figure 9. Cathodic polarization curve for armco iron in air-saturated aqueous 0.5M sodium chloride solution at 25°C; rotational speed of electrode = 0 rpm.

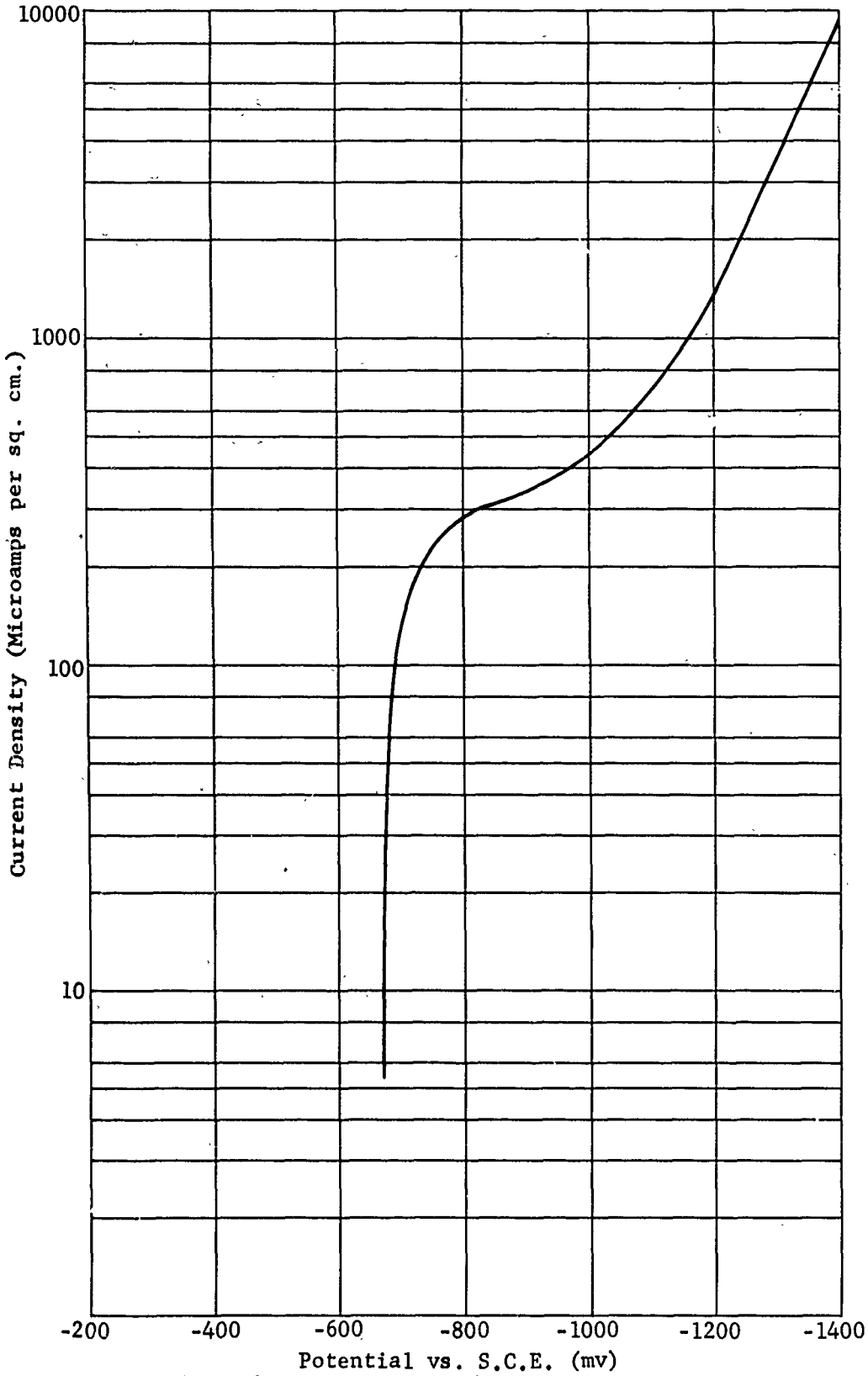

Figure 10. Cathodic polarization curve for armco iron in air-saturated aqueous 0.5M sodium chloride solution at 25°C; rotational speed of electrode = 100 rpm.

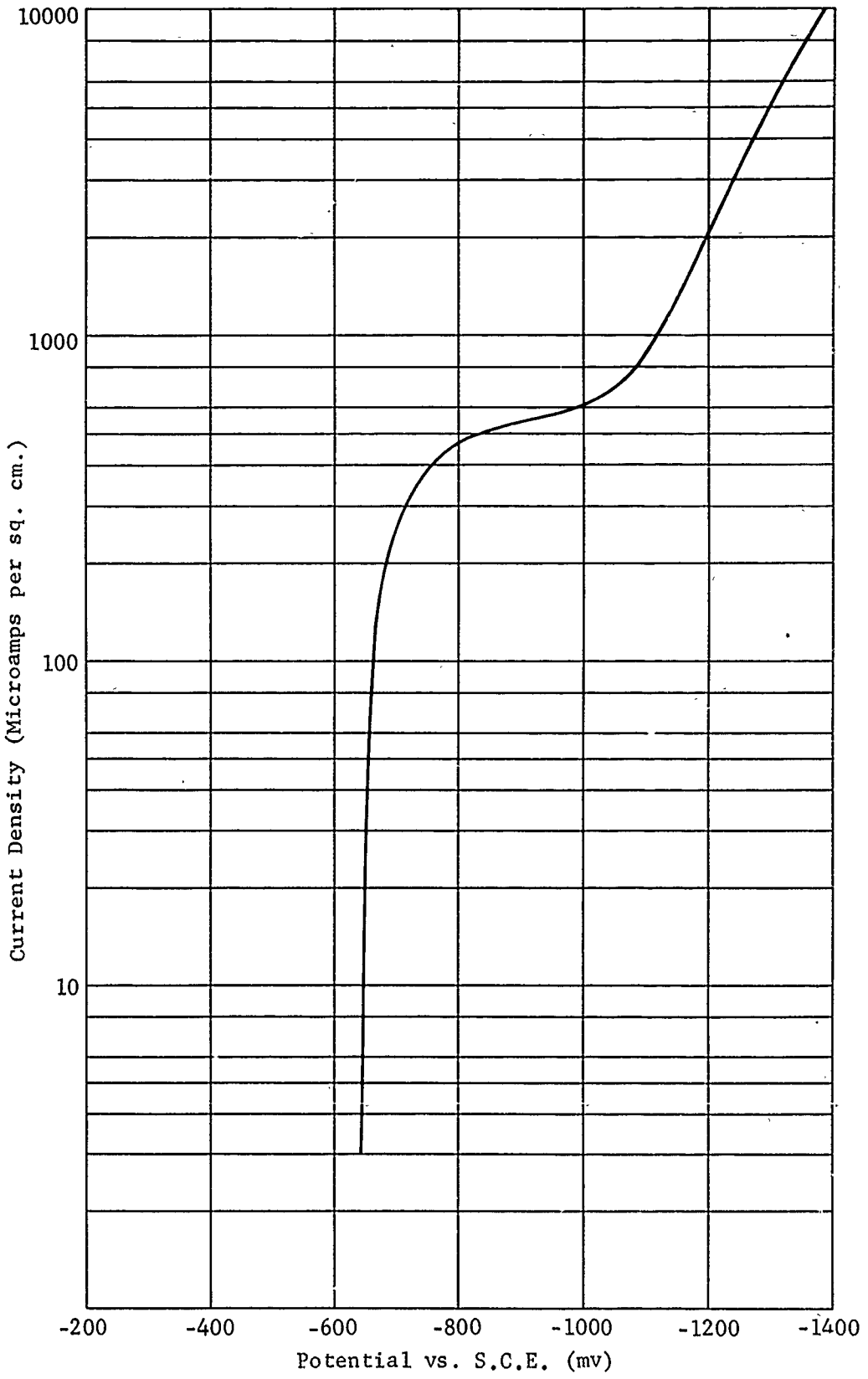

Figure 11. Cathodic polarization curve for armco iron in air-saturated aqueous 0.5M sodium chloride solution at 25°C; rotational speed of electrode = 400 rpm.

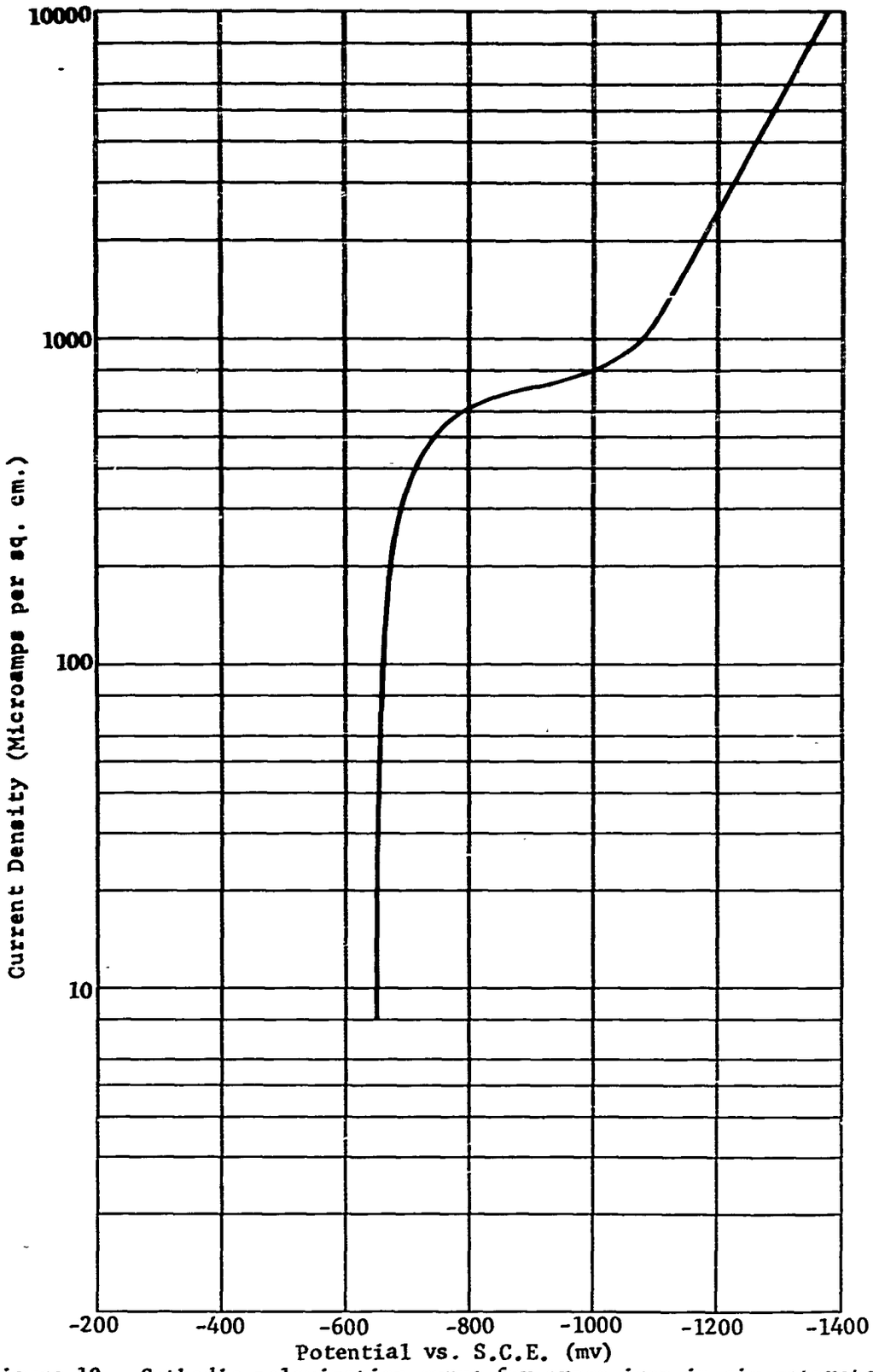

Figure 12. Cathodic polarization curve for armco iron in air-saturated aqueous 0.5M sodium chloride solution at 25°C; rotational speed of electrode = 900 rpm.

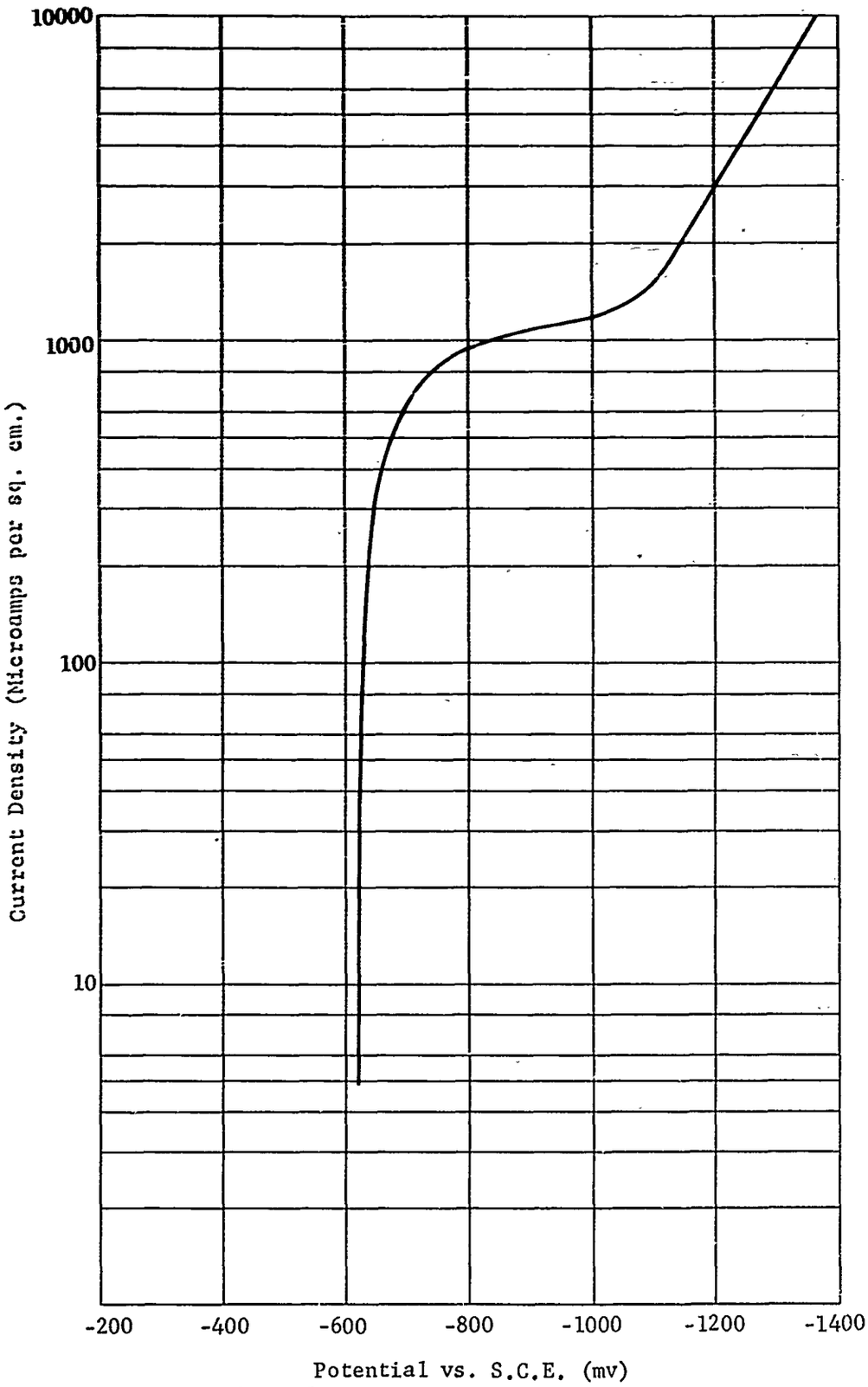

Figure 13. Cathodic polarization curve for armco iron in air-saturated aqueous 0.5M sodium chloride solution at 25°C; rotational speed of electrode = 1600 rpm.

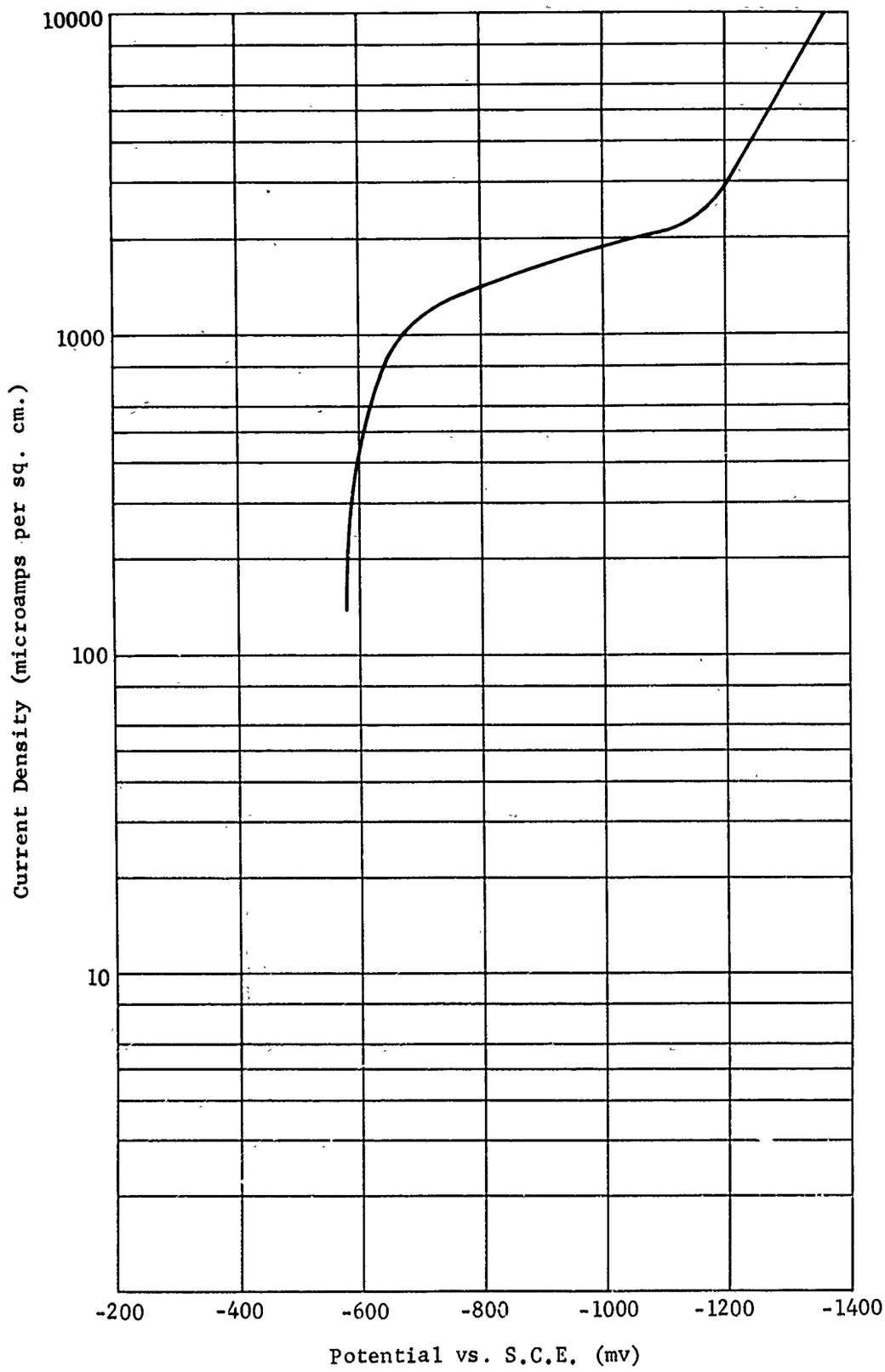

Figure 14. Cathodic polarization curve for armco iron in air-saturated aqueous 0.5M sodium chloride solution at 25°C: rotational speed of electrode = 2500 rpm.

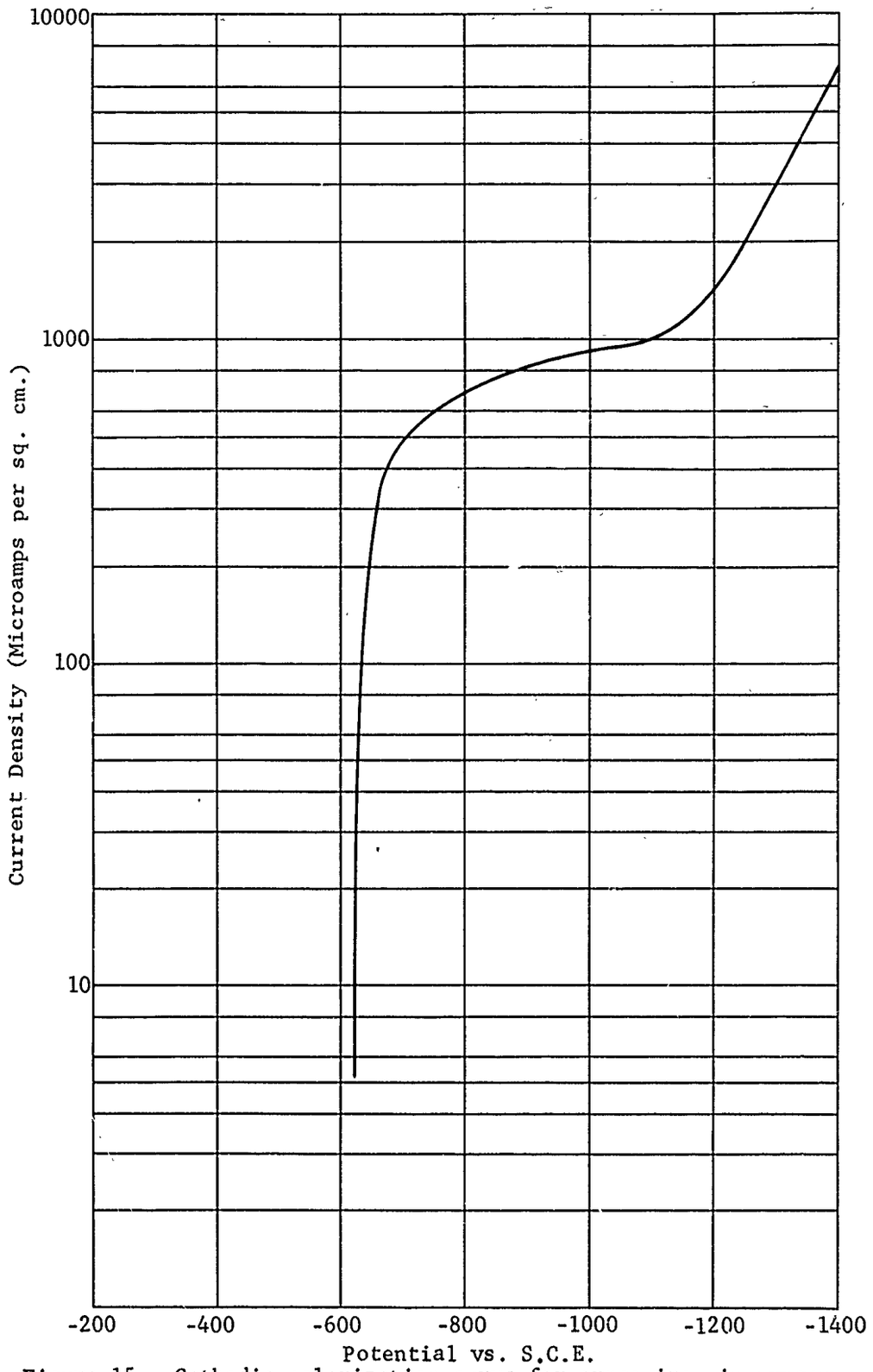

Figure 15. Cathodic polarization curve for armco iron in oxygen-saturated aqueous 0.5M sodium chloride solution at 25°C; rotational speed of electrode = 0 rpm.

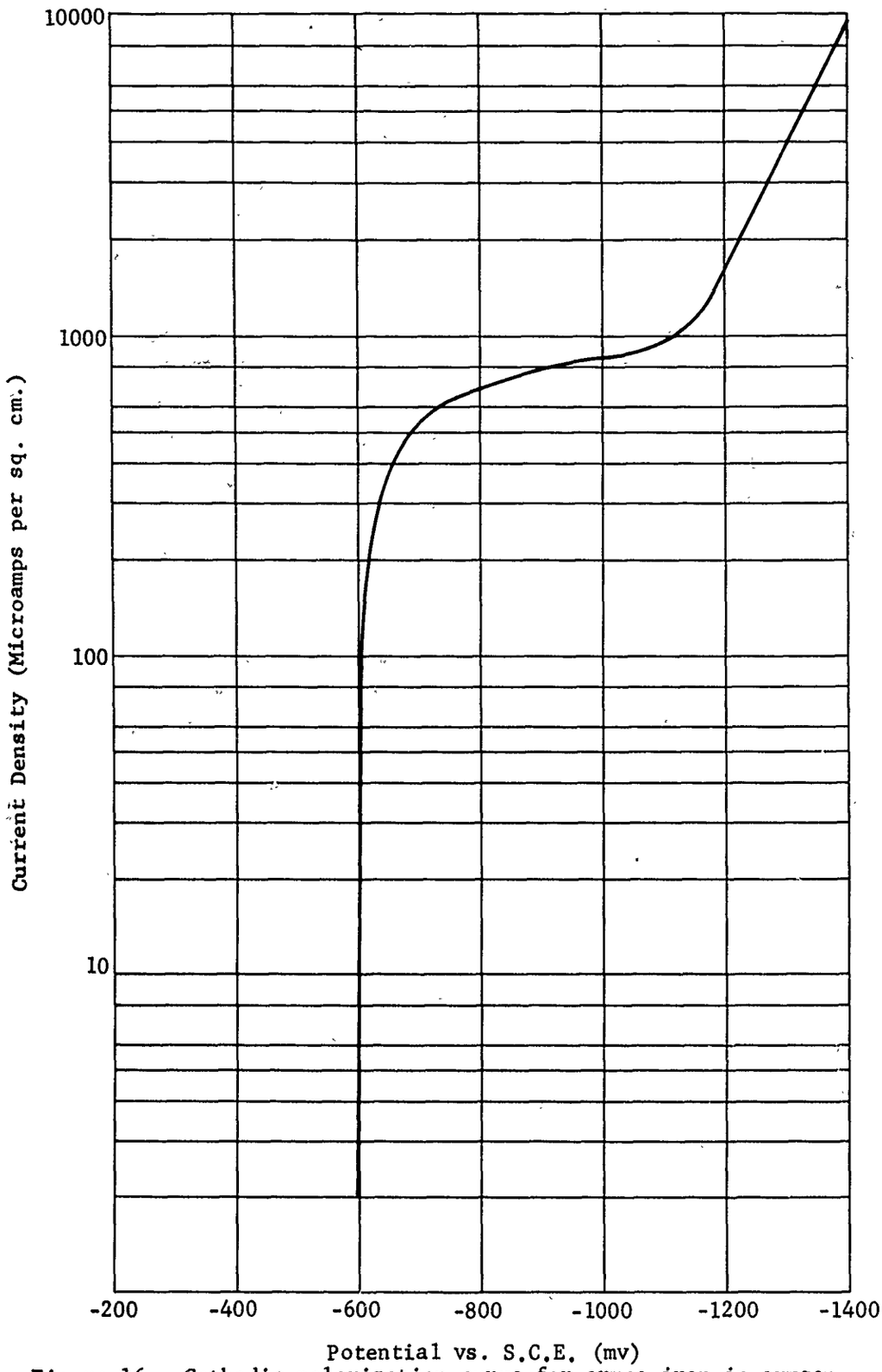

Figure 16. Cathodic polarization curve for armco iron in oxygen-saturated aqueous 0.5M sodium chloride solution at 25°C; rotational speed of electrode = 100 rpm.

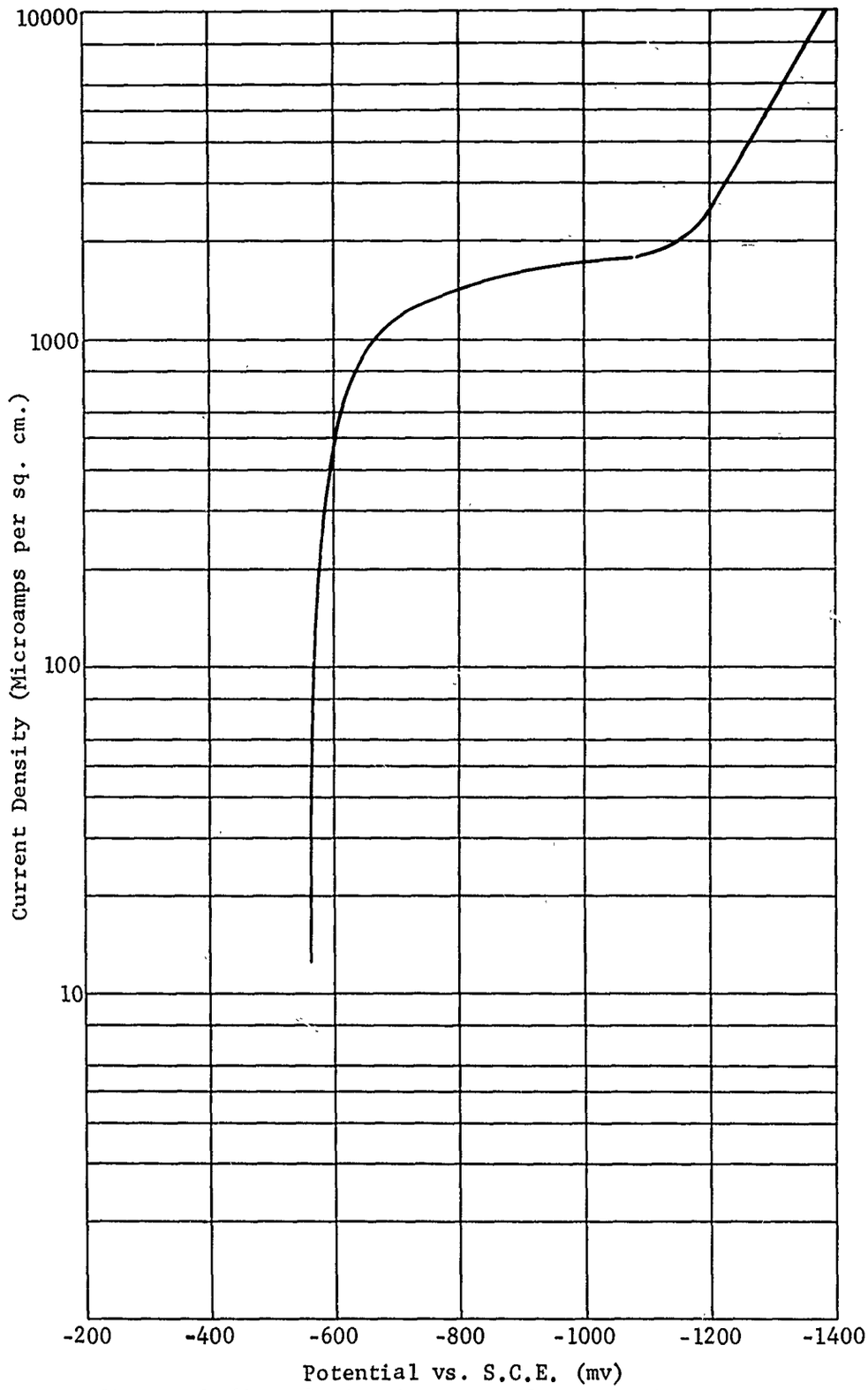

Figure 17. Cathodic polarization curve for armco iron in oxygen-saturated aqueous 0.5M sodium chloride solution at 25°C; rotational speed of electrode = 400 rpm.

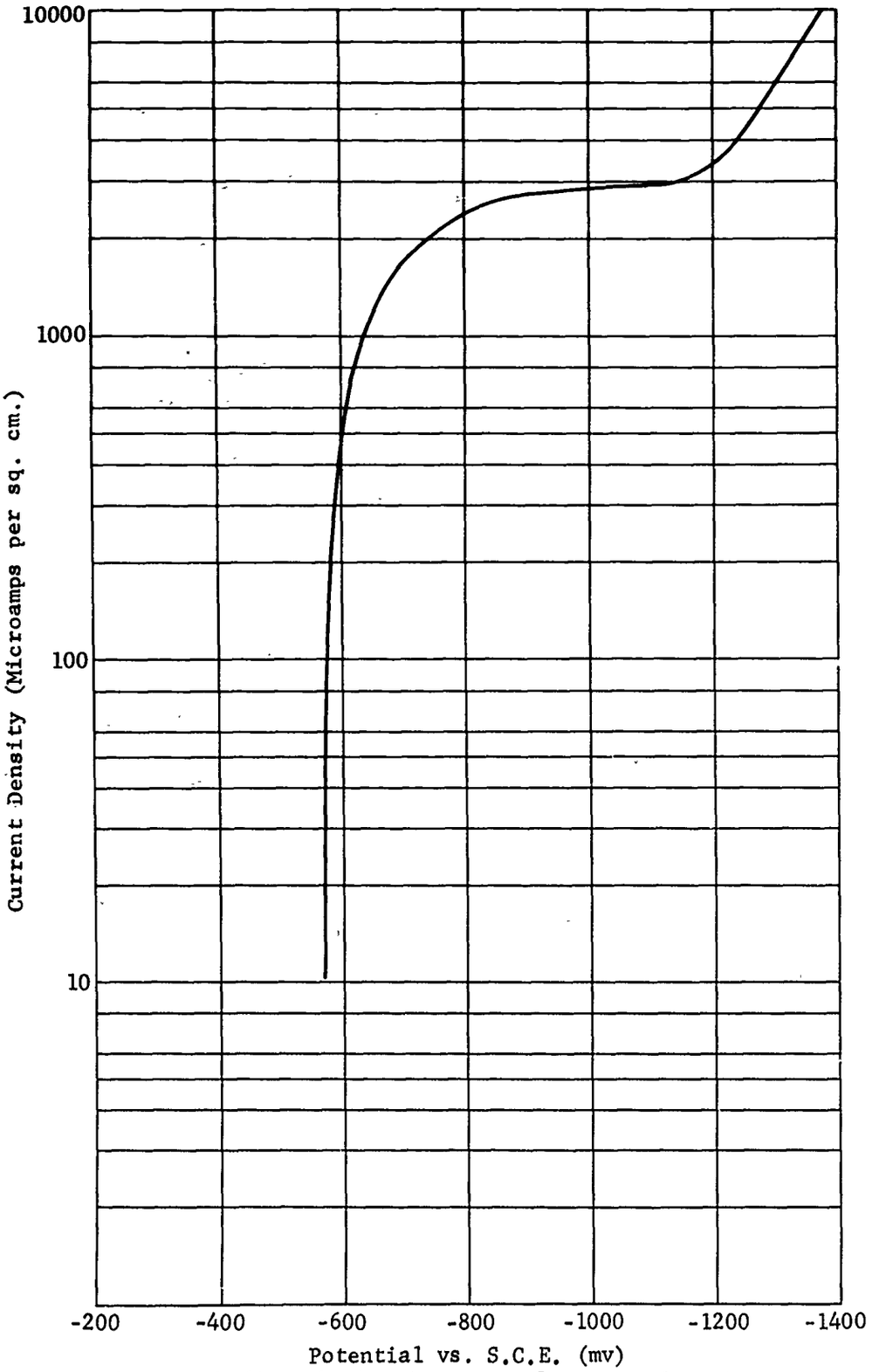

Figure 18. Cathodic polarization curve for armco iron in oxygen-saturated aqueous 0.5M sodium chloride solution at 25°C; rotational speed of electrode = 900 rpm.

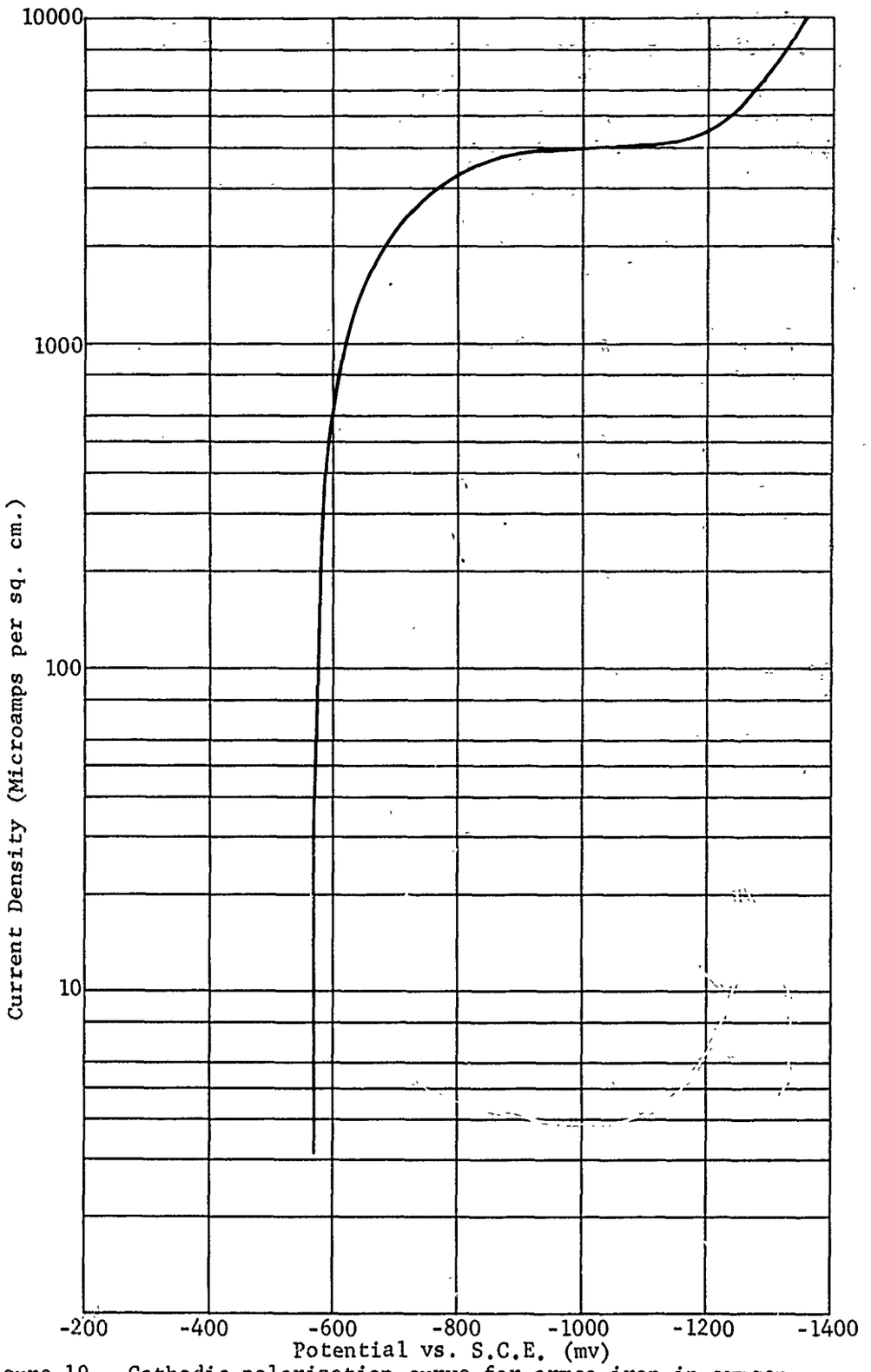

Figure 19. Cathodic polarization curve for armco iron in oxygen-saturated aqueous 0.5M sodium chloride solution at 25°C; rotational speed of electrode = 1600 rpm.

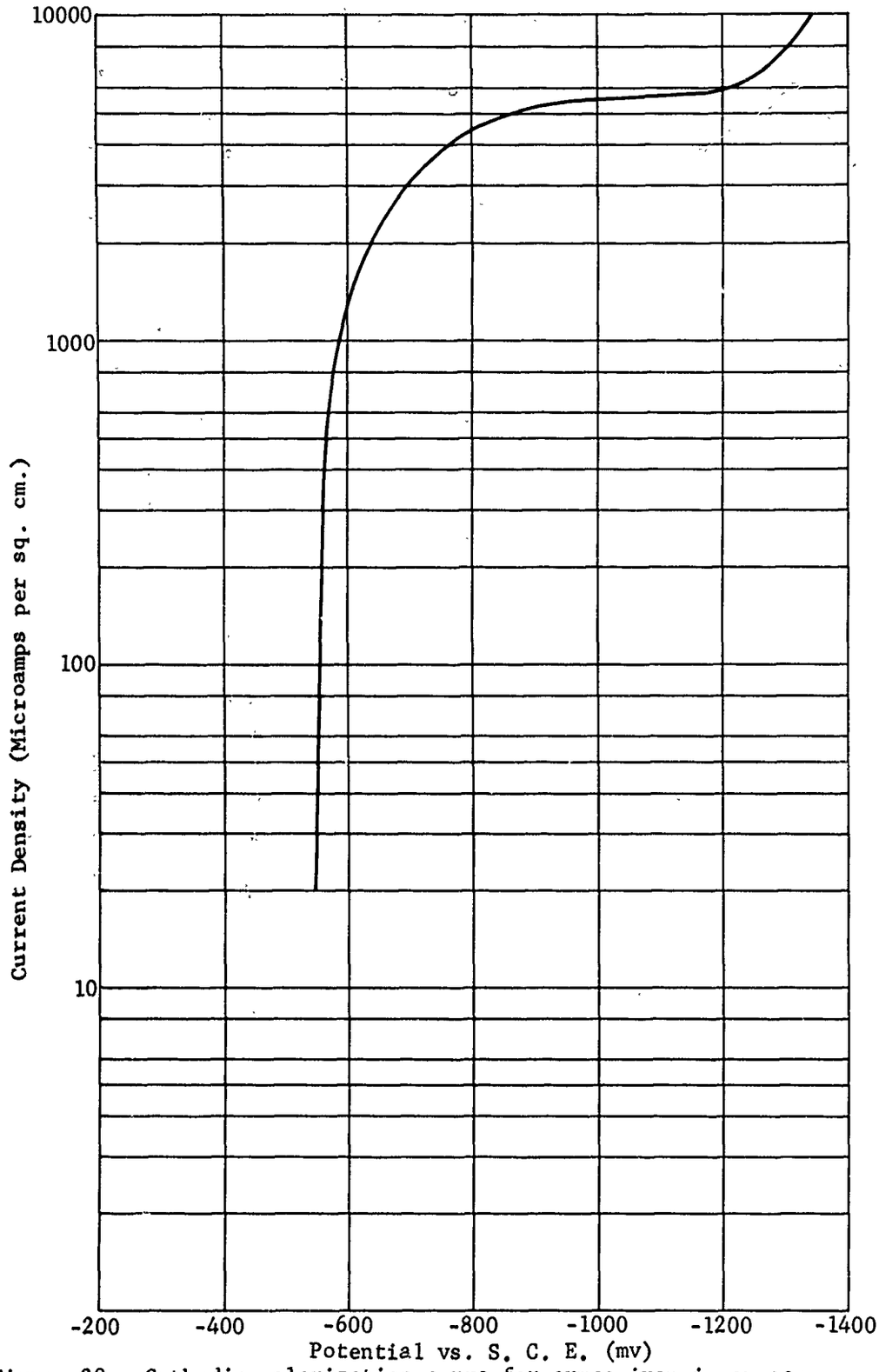

Figure 20. Cathodic polarization curve for armco iron in oxygen-saturated aqueous 0.5M sodium chloride solution at 25°C; rotational speed of electrode = 2500 rpm.

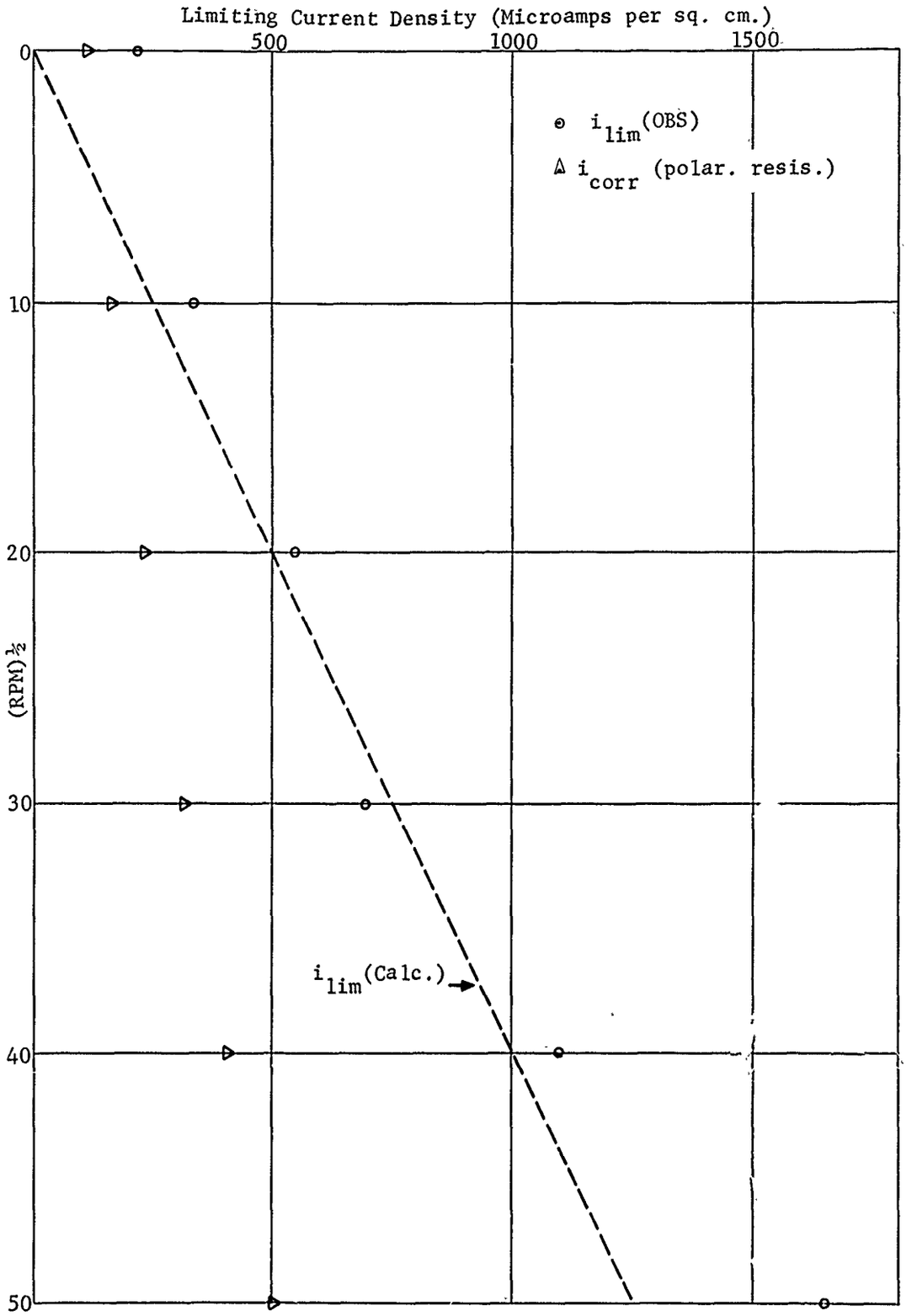

Figure 21. Limiting diffusion currents of armco iron in air-saturated aqueous 0.5M sodium chloride solution at 25°C as a function of the square root of angular velocity.

Table 1. Comparative Data from Experimental Runs on Armco Iron in Aqueous 0.5M Aqueous Sodium Chloride at 25°C.

Figure	Run	Saturated Gas	RPM	E_{corr}	$\Delta i/\Delta E$ μA/mv	C_{corr}(1) μA/cm^2	$i_{lim\ d}$ at -900 mv vs S.C.E., μa/cm^2
3	67-353-6	Nitrogen	0	-747	0.70	23	
4	67-353-2	Nitrogen	100	-751	1.27	42	
5	67-353-1	Nitrogen	400	-755	1.97	65	
6	67-353-3	Nitrogen	900	-743	0.93	31	
7	67-353-5	Nitrogen	1600	-730	1.05	35	
8	67-353-8	Nitrogen	2500	-712	1.41	46	
9	67-362-6	Air	0	-687	3.64	120	220
	67-361-7	Air	0	-694	3.29	109	230
10	67-362-7	Air	100	-666	5.02	166	340
	67-361-3	Air	100	-663	5.01	165	390
11	67-362-3	Air	400	-644	7.20	238	550
	67-362-2	Air	400	-620	7.64	252	600
12	67-362-5	Air	900	-650	9.58	316	700
	67-361-4	Air	900	-625	12.13	400	712
13	67-362-4	Air	1600	-618	12.32	406	1100
	67-361-6	Air	1600	-612	11.98	395	1020
14	67-362-8	Air	2500	-565	15.55	513	1650
	67-361-8	Air	2500	-599	16.79	554	1500

Cont'd.

Table 1. (Cont'd.)

Figure	Run	Saturated Gas	RPM	E_{corr}	$\Delta i/\Delta E$ μA/mv	C_{corr}(1) μA/cm^2	$i_{lim\ d}$ at -900 mv vs S.C.E., μA/cm^2
15	67-355-5	Oxygen	0	-623	13.65	447	880
16	67-355-2	Oxygen	100	-596	11.69	386	770
17	67-355-1	Oxygen	400	-559	16.36	540	1600
18	67-355-3	Oxygen	900	-568	23.37	772	2700
19	67-355-4	Oxygen	1600	-568	25.78	850	3800
20	67-355-6	Oxygen	2500	-546	31.89	1050	5200

(1) $\Delta E/\Delta I = \dfrac{B_a B_c}{2.3\ (i_{corr})\ (B_a + B_c)}$ $\quad B_a = 0.075V,\ B_c = \infty,\ i_{corr} = \dfrac{\Delta i}{\Delta E}$ (33.0)

Table 2. Limiting Diffusion Currents and Nernst Diffusion Layer Thickness, Calculated from the Levich Equation for Air-saturated 0.5M NaCl

RPM	R_n Reynolds Number	δ Nernst Diffusion Layer Thickness (cm)	$i_{lim\ d}$ Limiting Diffusion Current (μ a/cm^2)
100	4.2×10^2	0.0063	250
400	1.7×10^3	0.0032	500
900	3.8×10^3	0.0021	750
1600	6.7×10^3	0.0016	1000
2500	1.1×10^4	0.0013	1250

Unclassified
Security Classification

DOCUMENT CONTROL DATA - R & D

(Security classification of title, body of abstract and indexing annotation must be entered when the overall report is classified)

1. ORIGINATING ACTIVITY (Corporate author)
Naval Civil Engineering Laboratory
Port Hueneme, California 93041

2a. REPORT SECURITY CLASSIFICATION
Unclassified

2b. GROUP

3. REPORT TITLE
Corrosion of Iron in 0.5M NaCl - A Rotating Disk Electrode Study

4. DESCRIPTIVE NOTES (Type of report and inclusive dates)
Final - July 1967-January 1969

5. AUTHOR(S) (First name, middle initial, last name)
H. A. Porte

6. REPORT DATE
July 1969

7a. TOTAL NO. OF PAGES
32

7b. NO. OF REFS
0

8a. CONTRACT OR GRANT NO.

b. PROJECT NO. Z-R011-01-01-035

c.

d.

9a. ORIGINATOR'S REPORT NUMBER(S)
Technical Note N-1042

9b. OTHER REPORT NO(S) (Any other numbers that may be assigned this report)

10. DISTRIBUTION STATEMENT
Each transmittal of this document outside the agencies of the U. S. Government must have prior approval of the Naval Civil Engineering Laboratory.

11. SUPPLEMENTARY NOTES

12. SPONSORING MILITARY ACTIVITY
Director of Navy Laboratories
Washington, D. C.

13. ABSTRACT
The corrosion of iron was studied in 0.5 Molar sodium chloride solution by the rotating disk technique. Limiting diffusion currents were measured in nitrogen-saturated, air-saturated, and oxygen-saturated solutions at rotational speeds of 0, 100, 400, 900, 1600 and 2500 rpm. Corrosion potentials and corrosion rates at the corrosion potential were also determined. The observed limiting diffusion currents potential were also determined. The observed limiting diffusion currents showed good agreement with limiting diffusion currents calculated from the Levich theory for the rotating disk electrode. Measured corrosion rates (currents) were found to be lower than the limiting diffusion current, which is explained on the basis of a corrosion product film on the surface of the electrode.

DD FORM 1 NOV 65 1473 (PAGE 1)
S/N 0101-807-6801

Unclassified
Security Classification

Unclassified
Security Classification

14. KEY WORDS	LINK A ROLE	LINK A WT	LINK B ROLE	LINK B WT	LINK C ROLE	LINK C WT
Corrosion						
Iron						
Sodium Chloride						
Solutions						
Rotating disk electrode						
Electrodes						
Diffusion currents						

DD FORM 1 NOV 65 1473 (BACK)
(PAGE 2)

Unclassified
Security Classification